Korean J. Chem. Eng., 39(3), 499-503 (2022)
DOI: 10.1007/s11814-021-1005-z
pISSN: 0256-1115
eISSN: 1975-7220

RAPID COMMUNICATION

Reduced electrical hysteresis of organic thin-film transistors based on small molecule semiconductor through an insulating polymer binder

Soosang Chae*, Tae Il Lee,†, and Jin Young Oh***,†**

*IPF - Leibniz-Institut für Polymerforschung Dresden e.V, Institute of Physical Chemistry and Polymer Physics, 01069 Dresden, Germany
**Department of Materials Science and Engineering, Gachon University, Seongnam 13120, Korea
***Department of Chemical Engineering (Integrated Engineering Program), Kyung Hee University, Yongin 17104, Korea
(*Received 12 September 2021 • Revised 25 October 2021 • Accepted 4 November 2021*)

Abstract−The electrical stability of organic thin film transistors (OTFTs) based on 6, 13-bis(triisopropylsilylethynyl) (TIPS) pentacene were improved by blending poly(α-methylstyrene) (PαMS) binder with the TIPS-pentacene. The blended semiconducting film is vertically phase-separated, which forms a TIPS-pentacene rich region at top surface due to its lower surface energy than PαMS, inducing interface modification at semiconducting layer and dielectric layer. The modified interface induces an increase in charge current density and a decrease in charge trap density, leading to efficiently reduced electrical hysteresis and increased field-effect mobility.

Keywords: TIPS-pentacene, Vertical Phase Separation, Organic Thin Film Transistors

INTRODUCTION

Organic thin-film transistors (OTFTs) have received significant attention because of their intrinsic material advantages, such as mechanical flexibility and solution processability for expanding their applications with cost-effective fabrication technologies [1-4]. Recently, new strategies of molecular designs and material processing with functional materials have enabled the OTFTs to be intrinsically stretchable, self-healable, biodegradable for expanding their applications [5,6]. Moreover, field-effect mobility of OTFTs based on small molecule semiconductors has continuously increased over 30 cm^2/Vs with various scientific approaches [7,8]. 6, 13-bis(triisopropylsilylethynyl) pentacene (TIPS-pentacene) is one of the promising small molecule semiconductors for high performance OTFTS because of its high field-effect mobility, good solubility to various organic solvents, and high compatibility with electronic polymers [9,10].

Despite the merits of the OTFTs, electrical instability such as hysteresis of transfer characteristics, which leads to shift in the threshold voltage of the OTFTs, seriously limits commercialization of the OTFTs [11,12]. The hysteresis of OTFTs generally occurs due to charge carrier traps at the organic semiconductor-dielectric interface [13,14], slow polarization of the dielectric [15], and gate charge injection [16]. These reasons are closely associated with immobile stored negative charges at the semiconductor and dielectric interface, slow polarization of dipole groups inside the polymer dielectric materials, and trapped electrons in a vulnerable dielectric, respectively.

To reduce the hysteresis of the OTFTs, various concepts regarding interface engineering between semiconductor and dielectric have been suggested. Self-assembly monolayer (SAM) treatment on dielectric surface is one of presentative approaches for the dielectric interface engineering. Various functional groups of the SAM significantly affect the electrical performance of OTFTs. Recently, blending a small molecule semiconductor with an insulating polymer has been shown to further enhance mechanical flexibility as well as field-effect mobility of OTFTs [17-23]. The insulating polymers of low dielectric constant such as polystyrene, poly(perfluoroethylene-co-butenyl vinyl ether), and poly(α-methylstyrene) (PαMS) prevent the reduction of mobility originating from dipolar disorder [24,25]. Several research groups have reported that an organic semiconductor and polymer binder can undergo phase separation, which induces improving electrical characteristics [17-19,23]. However, the electrical stability of the blended semiconducting layer has not yet been sufficiently studied.

METHOD

In this paper, we report the electrical stability in terms of the hysteresis of OTFT with the semiconducting film blended of TIPS-pentacene and PαMS binder. The blended film was vertically phase-separated and a TIPS-pentacene rich region was formed at top surface due to its lower surface energy than PαMS. The phase separated semiconducting layer modified the semiconducting layer and dielectric interface, which significantly increased on-current with reduced charge trap density of the OTFTs, leading to higher field-effect mobility with efficiently reduced electrical hysteresis.

The top contact geometry was fabricated (channel length, L=80 μm and width, W=2,000 μm) on a highly doped p-type silicon substrate. A thermally grown SiO_2 was used as gate dielectric layer (200 nm) in order to exclude the hysteresis generated by the slow polarization in dielectric and gate charge injection. The source and

†To whom correspondence should be addressed.
E-mail: t2.lee77@gachon.ac.kr, jyoh@khu.ac.kr

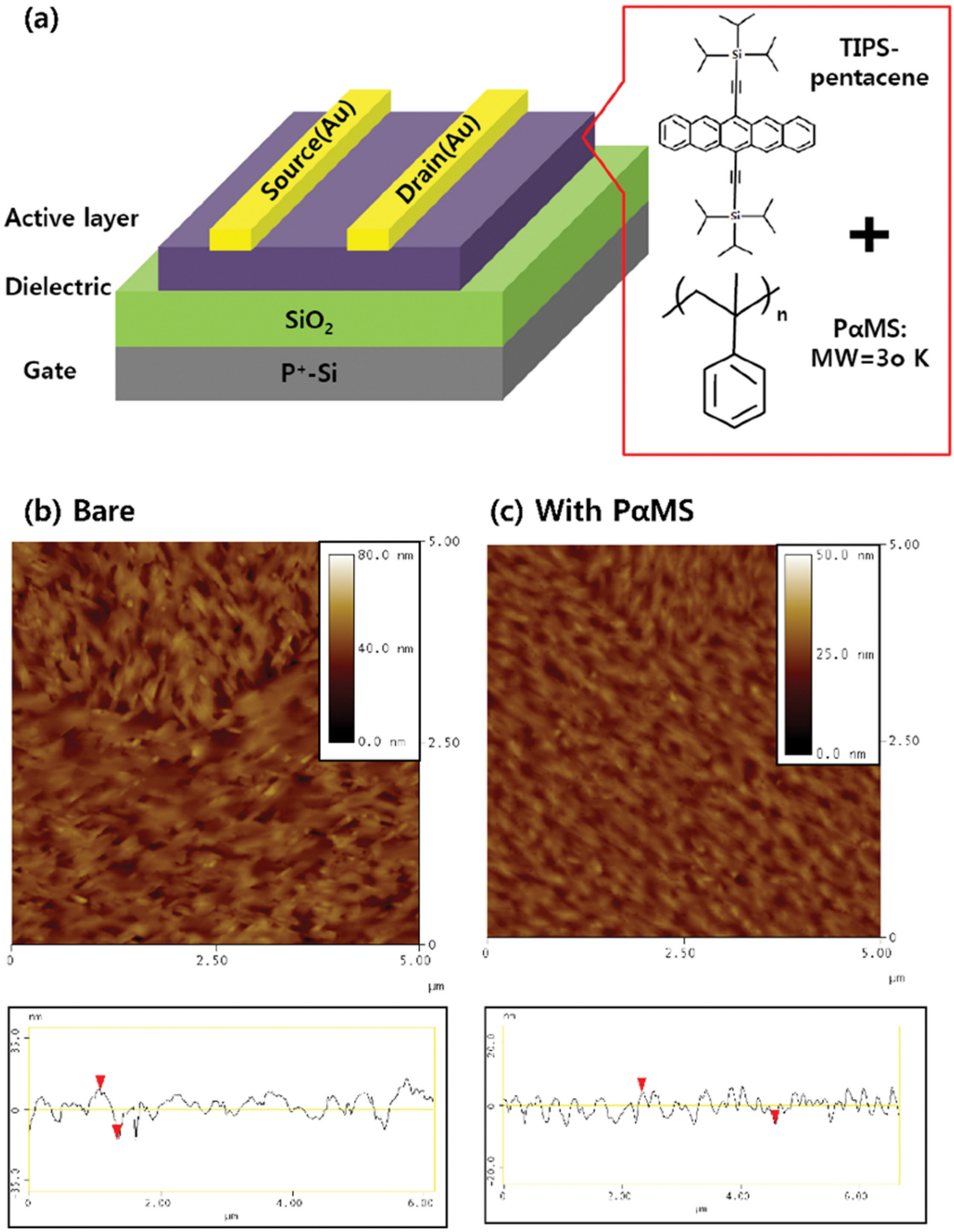

Fig. 1. (a) Schematic illustration of TIPS-pentacene organic thin film transistors (OTFTs) using polymer binder (PαMS). AFM images of OTFTs with (b) bare TIPS-pentacene film (c) blended semiconducting film. RMS roughness values of bare TIPS-pentacene film and blended film are 5.61 nm and 2.99 nm, respectively.

drain electrodes (Au) with a thickness of 100 nm were deposited by thermal evaporation. The solutions of TIPS-pentacene (bare TIPS-pentacene) and TIPS-pentacene blended with PαMS (blended TIPS-pentacene) in chrolobenzene were deposited by spin coating from a 1 wt% onto the SiO_2 dielectric layer. The blend weight ratio of TIPS-pentacene and PαMS was 1 : 1. The samples were then heated on a hot plate at 90 °C for 20 min. After fabrication of the OTFTs devices, the electrical characteristics were measured by a semiconductor parameter analyzer (Agilent 5270B) under ambient air at room temperature at the Core Facility Center for Analysis of Optoelectronic Materials and Devices of the Korea Basic Science Institute (KBSI).

Fig. 1(a) shows the schematic structure of OTFTs. The morphology of the bare TIPS-pentacene and blended TIPS-pentacene active layers was observed by atomic force microscopy (AFM). Fig. 1(b) and 1(c) show AFM images of bare TIPS-pentacene and blended

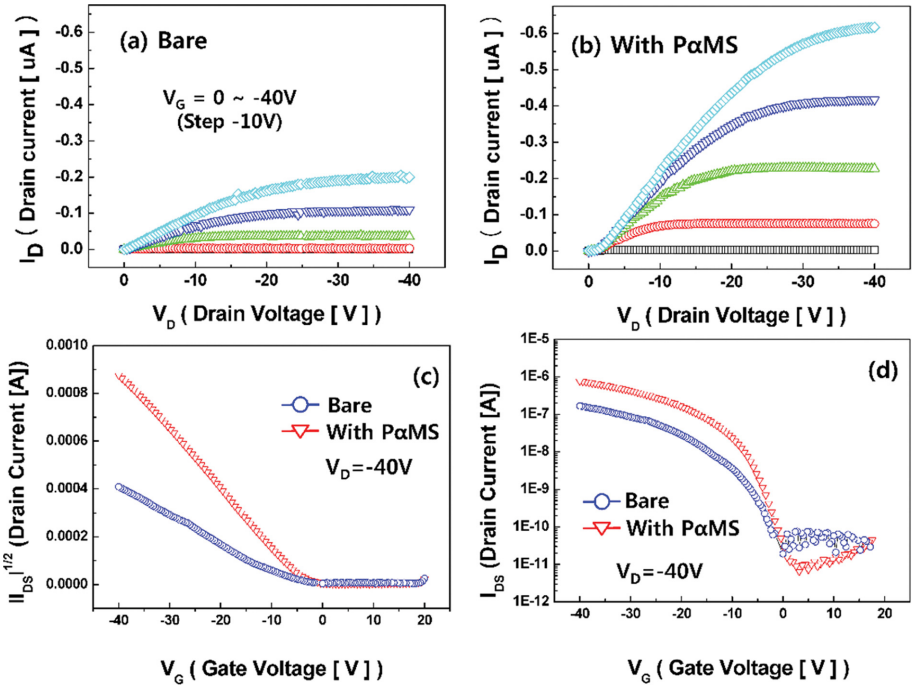

Fig. 2. I_D-V_D curves at various V_G obtained from OTFTs using (a) bare TIPS-pentacene layer, (b) blended TIPS-pentacene/PαMS layer. (c) $\sqrt{I_D}$-V_G and (d) Log_{10} (I_D)-V_G curves for the estimation of saturation regime mobility that were obtained at V_D=−40 V from TIPS-pentacene based OTFTs (channel length, L=80 μm and channel width, W=2,000 μm).

TIPS-pentacene films, deposited on thermally grown SiO_2 substrates, respectively. The bare film showed a higher root mean square (RMS) of 5.6 nm compared to that of blended film which was smoothed to 2.9 nm. This improved flatness of the semiconducting film is due to the PαMS polymer binder, which is expected to enhance the interface uniformity in large area between the active layer and electrode [18,20,26].

The output and transfer characteristics are shown in Fig. 2(a)-(d) for the OTFTs. The OTFT devices exhibited typical curves of p-type OTFTs working in an accumulation mode. Fig. 2(a) and 2(b) show the output characteristics bare TIPS-pentacene and blended TIPS-pentacene, respectively. Both OTFTs were normally operated at lower gate voltage than −40 V and the maximum saturation current of the OTFT fabricated with blended TIPS-pentacene showed three-times higher than the OTFT with bare TIPS-pentacene. The field effect mobility was determined from the $\sqrt{I_D}$-V_G curves, as shown in Fig. 2(c) and 2(d). The mobility for the bare and blended TIPS-pentacene OTFTs was 7.3×10^{-4} and 2.7×10^{-3} cm^2/Vs, respectively. The extracted threshold voltage (V_{th}) was −6.6 V for the bare OTFT, while V_{th} for the blended OTFTs was shifted to positive direction. The on/off current ratio for bare and blended OTFTs was 4×10^3 and 1×10^5, respectively, as shown in Fig. 2(d). These improved electrical characteristics of the blended OTFT are closely related to the morphology of active layer. The well-ordered TIPS-pentacene molecules in active region of semiconducting film resulted in the formation of a device with high mobility, high on/off ratios, and a threshold voltage near to zero voltage. In contrast, the disordered TIPS-pentacene film resulted in a device in which the mobility, on/off ratio and threshold voltage were relatively lower [27].

To examine crystallinity of the semiconducting films, X-ray diffraction (XRD) analysis was performed at the Core Facility for Bionano Materials in Gachon University because crystallinity significantly affects the charge transport in conjugated molecules, as shown in Fig. 3. The pure TIPS-pentacene and PαMS show the

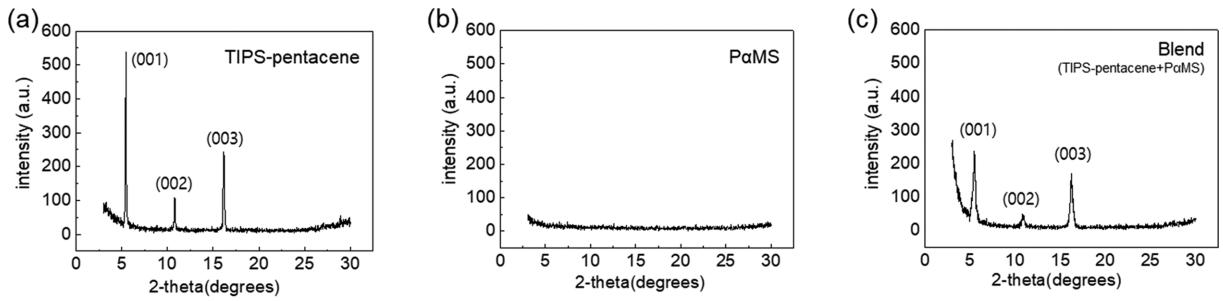

Fig. 3. XRD diffractograms of (a) pure TIPS-pentacene, (b) pure PαMS, and (c) TIPS-pentacene/PαMS blended film.

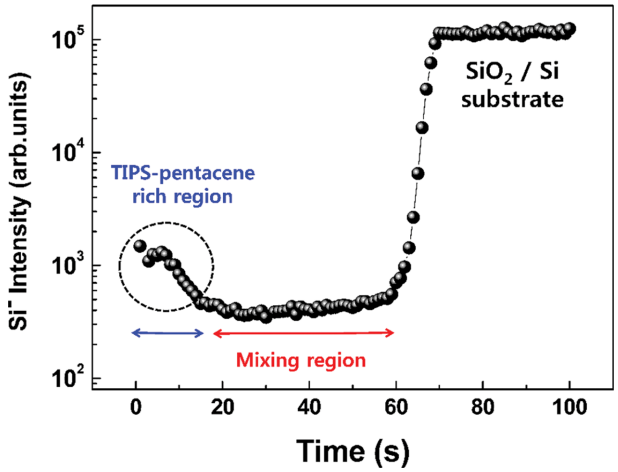

Fig. 4. Depth profile of Si^- ions in a TIPS-pentacene/PαMS blended film.

typical crystalline and amorphous diffraction pattens, respectively (Fig. 3(a) and 3(b)). The blend film has lower crystallinity than that of the pure TIPS-pentacene, which implies the improved electrical performance of the blended film is closely related with the interface between semiconducting layer and dielectric.

To evaluate the interface, the vertical composition of TIPS-pentacene molecules in the blended semiconducting film was investigated using a time-of-flight secondary ion mass spectrometer (TOF-SIMS). The blended film was vertically separated into two regions (TIPS-pentacene rich region/mixing region) as shown in Fig. 4. While the active channel is formed between TIPS-pentacene and SiO_2 dielectric layer for bare TIPS-pentacene OTFT, in case of blended system, the two regions in semiconducting film can serve as the active region (TIPS-pentacene rich region) for transport charges and the active assistance region (mixing region) for the modification of the interface at semiconducting layer and SiO_2 dielectric layer. Because the most TIPS-pentacene is phase separated at the top region, the bottom mixing region seems not to be an effective active layer. The higher surface energy of PαMS than TIPS-pentacene and almost same surface energy of pure TIPS-pentacene and blended film as shown in Table 1 support vertical phase separation forming TIPS-pentacene rich region at top surface.

From point of resistance, the mixing layer is supposed to serve as a resistor; therefore, the most current in the semiconducting layer should flow though the TIPS-pentacene rich region. Consequently, we suggest that a modified interface is generated between the semiconducting layer and dielectric interface. The property of TIPS-pentacene near the TIPS-pentacene rich region/mixing region interface

Table 1. Contact angles and surface energy of TIPS-pentacene, PαMS, and TIPS-pentacene/PαMS blend film

Materials	Water angle (°)	Diiodomethane angle (°)	Surface energy (mJ/m^2)
PαMS	99.46	27.69	45.81
TIPS-pentacene	102.17	36.26	42.15
Blend film	104.30	35.48	42.94

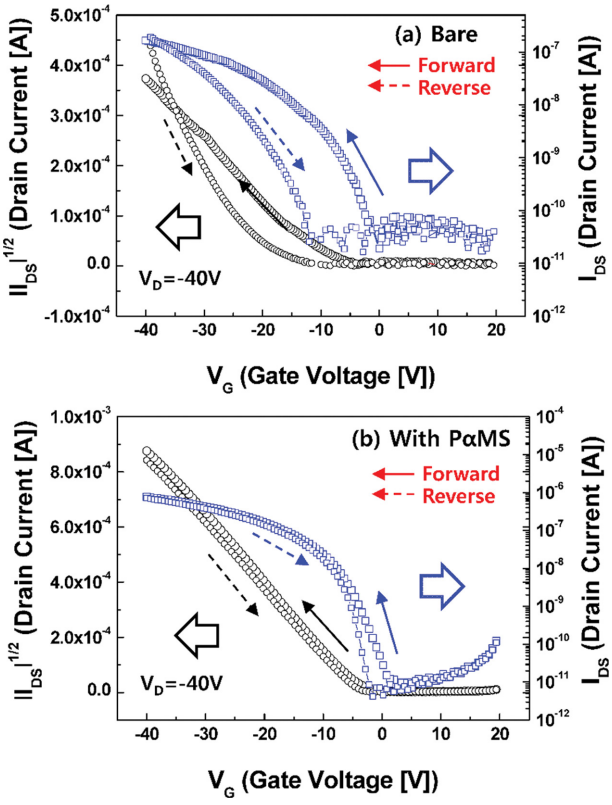

Fig. 5. $\sqrt{I_D}$-V_G and Log_{10} (I_D)-V_G transfer curves of OTFTs using bare TIPS pentacene and blended TIPS-pentacene/PαMS film. The gate voltage was swept forward and then backward.

might also be improved [17]. Accordingly, the OTFTs using TIPS-pentacene with PαMS improved carrier transport without any leakage current, as shown in Fig. 2(d). From this point of view, the polymer blend gives rise to improvement of electrical characteristics [22,23].

To confirm the electrical stability of the OTFTs, we determined the hysteresis behavior of the current-voltage (I-V) curves, as shown in Fig. 5. The gate-to-source voltage (V_{GS}) was continuously swept in steps of 0.4 V, starting from +20 V, passing through −40 V, and finally arriving at +20 V again. The bare TIPS-pentacene OTFTs exhibited tremendous hysteresis shown in Fig. 5(a). The threshold voltage was shifted from −6.6 to −18.2 V. On the other hand, the hysteresis of the blended OTFTs was significantly reduced with the slight threshold voltage shift (−1.2 V) from −3.7 to −4.9 V as shown in Fig. 5(b). Interestingly, the direction of threshold voltage shift was the same anticlockwise direction in both devices, which is attributed to the charge carrier trapping at the organic semiconductor-dielectric interface [19]. This phenomenon is different from the polar nature of adsorbed water at the organic semiconductor-dielectric interface or charge injection from the gate, where a positive threshold voltage shift (clockwise) is expected [28,29].

The reduced hysteresis of the OTFT with the blended semiconducting film might be due to the PαMS insulating binder of the mixing region in the semiconducting film, which passivates hydroxyl groups (-OH) at the SiO_2 dielectric surface because oxide dielectrics generally contain a high density of -OH groups serving as trap

sites on their top surface [30].

Another way to represent carrier charge trap density is by the sub-threshold slope (SS) because the SS represents the carrier charge trap density of the OTFTs [31,32]. The SS values of bare TIPS-pentacene and blended TIPS-pentacene devices were 4.1 V/decade and 2.5 V/decade, respectively. The improvement in the characteristics of the sub-threshold slope and the threshold voltage shift indicated a decreased charge trap density of the blended OTFTs. The charge trap density (Nt) calculated from SS values of the bare and blended films was 7.36×10^{12} cm^{-2} eV^{-1} and 4.44×10^{12} cm^{-2} eV^{-1}, respectively. The reduced charge trap density thus led to decreased hysteresis behavior of the device. Therefore, the vertical phase separation of the semiconducting layer blended with an insulating polymer binder improved the device performance with electrical stability.

CONCLUSION

We demonstrated reduced hysteresis of small molecule based OTFT by blending TIPS-pentacene semiconductor and insulating PαMS binder. The blended semiconducting layer was vertically separated into TIPS-pentacene rich top region and mixing bottom region due to surface energy differences of both materials. The relatively insulating bottom mixing region modified the semiconducting layer and dielectric interface, which efficiently reduced charge trap density, leading to significantly reduced electrical hysteresis of the OTFT device. We hope that the results may pave the way forward for more efficient strategies to optimize the vertical phase separation of conducting and semiconducting organic materials in various application fields, such as organic photovoltaics, flexible sensors, and printable electronic devices.

ACKNOWLEDGEMENT

This work was supported by a grant from Kyung Hee University in 2018 (KHU-20182218). Also, this work was supported by the Gachon University research fund of 2018 (GCU-2018-0364).

REFERENCES

1. J. Y. Oh, S. Rondeau-Gagné, Y.-C. Chiu, A. Chortos, F. Lissel, G.-J. N. Wang, B. C. Schroeder, T. Kurosawa, J. Lopez, T. Katsumata, J. Xu, C. Zhu, X. Gu, W.-G. Bae, Y. Kim, L. Jin, J. W. Chung, J. B. H. Tok and Z. Bao, *Nature*, **539**, 411 (2016).
2. J. Xu, S. Wang, G.-J. N. Wang, C. Zhu, S. Luo, L. Jin, X. Gu, S. Chen, V. R. Fei, J. W. F. To, S. Rondeau-Gagné, J. Park, B. C. Schroeder, C. Lu, J. Y. Oh, Y. Wang, Y.-H. Kim, H. Yan, R. Sinclair, D. Zhou, G. Xue, B. Murmann, C. Linder, W. Cai, J. B.-H. Tok, J. W. Chung and Z. Bao, *Science*, **355**, 59 (2017).
3. J. Y. Oh, D. Son, T. Katsumata, Y. Lee, Y. Kim, J. Lopez, H.-C. Wu, J. Kang, J. Park, X. Gu, J. Mun, N. G.-J. Wang, Y. Yin, W. Cai, Y. Yun, J. B. H. Tok and Z. Bao, *Sci. Adv.*, **5**, eaav3097 (2019).
4. S. Wang, J. Xu, W. Wang, G. N. Wang, R. Rastak, F. Molina-Lopez, J. W. Chung, S. Niu, V. R. Feig, J. Lopez, T. Lei, S. K. Kwon, Y. Kim, A. M. Foudeh, A. Ehrlich, A. Gasperini, Y. Yun, B. Murmann, J. B. Tok and Z. Bao, *Nature*, **555**, 83 (2018)
5. S. Wang, J. Y. Oh, J. Xu, H. Tran and Z. Bao, *Acc. Chem. Res.*, **5**, 1033 (2018).
6. J. Y. Oh and Z. Bao, *Adv. Sci.*, **6**, 1900186 (2019)
7. H. Minemawari, T. Yamada, H. Matsui, J. Tsutsumi, S. Haas, R. Chiba, R. Kumai and T. Hasegawa, *Nature*, **475**, 364 (2011).
8. Y. Yuan, G. Giri, A. L. Ayzner, A. P. Zoombelt, S. C. B. Mannsfeld, J. Chen, D. Nordlund, M. F. Toney, J. Huang and Z. Bao, *Nat. Commun.*, **5**, 3005 (2014).
9. D. H. Kim, D. Y. Lee, H. S. Lee, W. H. Lee, Y. H. Kim, J. I. Han and K. Cho, *Adv. Mater.*, **19**, 678 (2007).
10. Y. Diao, B. C.-K. Tee, G. Giri, J. Xu, D. H. Kim, H. A. Becerril, R. M. Stoltenberg, T. H. Lee, G. Xue, S. C. B. Mannsfeld and Z. Bao, *Nat. Mater.*, **12**, 665 (2013).
11. W. Huang, W. Shi, S. Han and J. Yu, *AIP Adv.*, **3**, 052122 (2013).
12. M. Egginger, S. Bauer, R. Schwödiauer, H. Neugebauer and N. S. Sariciftci, *Monatsh. Chem.*, **140**, 735 (2009).
13. D. K. Hwang, M. S. Oh, J. M. Hwang, J. H. Kim and S. Im, *Appl. Phys. Lett.*, **92**, 013304 (2008).
14. G. Gu, M. G. Kane, J. E. Doty and A. H. Firester, *Appl. Phys. Lett.*, **87**, 243512 (2005).
15. J.-Y. Kim, J. W. Kim, E. K. Lee, J.-I. Park, B.-L. Lee, Y.-N. Kwon, S. Byun, M.-S. Jung and J.-J. Kim, *J. Mater. Chem. C*, **6**, 13359 (2006).
16. C. A. Lee, D. W. Park, S. H. Jin, I. H. Park, J. D. Lee and B.-G. Park, *Appl. Phys. Lett.*, **88**, 252102 (2006).
17. L. Qiu, J. A. Lim, X. Wang, W. H. Lee, M. Hwang and K. Cho, *Adv. Mater.*, **20**, 1141 (2008).
18. T. Ohe, M. Kuribayashi, R. Yasuda, A. Tsuboi, K. Nomoto, K. Satori, M, Itabashi and J. Kasahara, *Appl. Phys. Lett.*, **93**, 053303 (2008).
19. J. Kang, N. Shin, D. Y. Jang, V. M. Prabhu and D. Y. Yoon, *J. Am. Chem. Soc.*, **130**, 12273 (2008).
20. J. H. Kwon, S. Shin, S. Kim, M. J. Cho, K. N. Kim, D. H. Choi and B. Ju, *Appl. Phys. Lett.*, **94**, 013506 (2009).
21. M.-B. Madec, P. J. Smith, A. Malandraki, N. Wang, J. G. Korvink and S. G. Yeates, *J. Mater. Chem.*, **20**, 9155 (2010).
22. L. Qiu, W. H. Lee, Z. Whang, J. S. Kim, J. A. Lim, D. Kwak, S. Lee and K. Cho, *Adv. Mater.*, **21**, 1349 (2009).
23. W. H. Lee, J. A. Lim, D. Kwak, J. H. Cho, H. S. Lee, H. H. Choi and K. Cho, *Adv. Mater.*, **21**, 4243 (2009).
24. J. Veres, S. Ogier, S. W. Leeming, D. C. Cupertino and S. M. Khaffaf, *Adv. Funct. Mater.*, **13**, 199 (2003).
25. A. Babel and S. A. Jenekhe, *Macromolecules*, **37**, 9835 (2004).
27. C. Yang, K. Shin, S. Y. Yang, H. Jeon, D. Choi, D. S. Chung and C. E. Park, *Appl. Phys. Lett.*, **89**, 153508 (2006).
28. C. S. Kim, S. Lee, E. D. Gomez, J. E. Anthony and Y. L. Loo, *Appl. Phys. Lett.*, **93**, 103302 (2008).
29. L. L. Chua, J. Zaumseil, J. F. Chang, E. C. W. Ou, P. H. K. H. Ho, H. Sirringhaus and R. H. Friend, *Nature,* **434**, 194 (2005).
30. C. S. Kim, S. J. Jo, S. W. Lee, W. J. Kim, S. H. Lee and H. K. Baik, *Adv. Funct. Mater.*, **17**, 958 (2007).
31. A. Rolland, J. Richard, J. P. Kleider and D. Mencaraglia, *J. Electrochem. Soc.*, **140**, 3679 (1993).
32. M. McDowell, I. G. Hill, J. E. McDermott, S. L. Bernasek and J. Schwarts, *Appl. Phys. Lett.*, **88**, 073505 (2006).